Since January 2020 Elsevier has created a COVID-19 resource centre with free information in English and Mandarin on the novel coronavirus COVID-19. The COVID-19 resource centre is hosted on Elsevier Connect, the company's public news and information website.

Gastroenterology 2022;163:495–506

Postacute COVID-19 is Characterized by Gut Viral Antigen Persistence in Inflammatory Bowel Diseases

Andreas Zollner,[1,*] **Robert Koch**,[1,*] Almina Jukic,[1] Alexandra Pfister,[1] Moritz Meyer,[1] Annika Rössler,[2] Janine Kimpel,[2] **Timon E. Adolph**,[1,§] and **Herbert Tilg**[1,§]

[1]Department of Internal Medicine I, Gastroenterology, Hepatology, Endocrinology & Metabolism, Medical University of Innsbruck, Innsbruck, Austria; and [2]Department of Hygiene, Microbiology and Public Health, Institute of Virology, Medical University of Innsbruck, Innsbruck, Austria

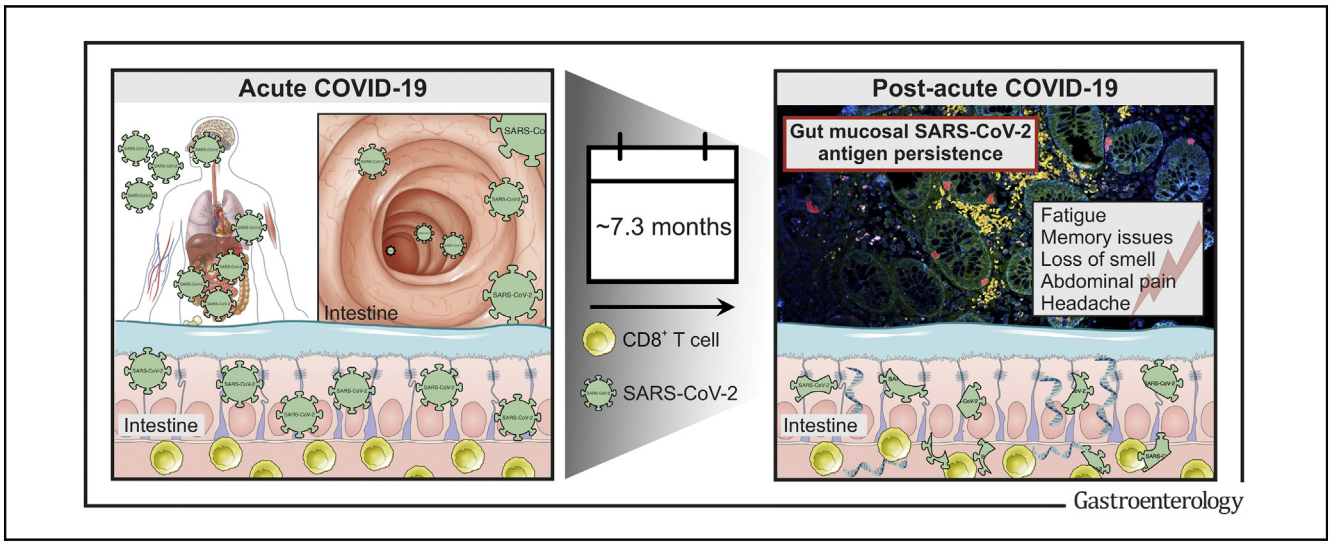

See editorial on page 376.

BACKGROUND & AIMS: The coronavirus disease 2019 (COVID-19) pandemic has affected populations, societies, and lives for more than 2 years. Long-term sequelae of COVID-19, collectively termed the postacute COVID-19 syndrome, are rapidly emerging across the globe. Here, we investigated whether severe acute respiratory syndrome coronavirus 2 (SARS-CoV-2) antigen persistence underlies the postacute COVID-19 syndrome. **METHODS:** We performed an endoscopy study with 46 patients with inflammatory bowel disease (IBD) 219 days (range, 94–257) after a confirmed COVID-19 infection. SARS-CoV-2 antigen persistence was assessed in the small and large intestine using quantitative polymerase chain reaction of 4 viral transcripts, immunofluorescence of viral nucleocapsid, and virus cultivation from biopsy tissue. Postacute COVID-19 was assessed using a standardized questionnaire, and a systemic SARS-CoV-2 immune response was evaluated using flow cytometry and enzyme-linked immunosorbent assay at endoscopy. IBD activity was evaluated using clinical, biochemical, and endoscopic means. **RESULTS:** We report expression of SARS-CoV-2 RNA in the gut mucosa ~7 months after mild acute COVID-19 in 32 of 46 patients with IBD. Viral nucleocapsid protein persisted in 24 of 46 patients in gut epithelium and $CD8^+$ T cells. Expression of SARS-CoV-2 antigens was not detectable in stool and viral antigen persistence was unrelated to severity of acute COVID-19, immunosuppressive therapy, and gut inflammation. We were unable to culture SARS-CoV-2 from gut tissue of patients with viral antigen persistence. Postacute sequelae of COVID-19 were reported from the majority of patients with viral antigen persistence, but not from patients without viral antigen persistence. **CONCLUSION:** Our results indicate that SARS-CoV-2 antigen persistence in infected tissues serves as a basis for postacute COVID-19. The concept that viral antigen persistence instigates immune perturbation and postacute COVID-19 requires validation in controlled clinical trials.

Keywords: SARS-CoV-2; COVID-19; Postacute COVID-19; Viral Antigen Persistence.

***Authors share co-first authorship. §Authors share co-senior authorship.**

Abbreviations used in this paper: **ACE2, angiotensin-converting enzyme 2; COVID-19, coronavirus disease 2019; ELISA, enzyme-linked immunosorbent assay; IBD, inflammatory bowel disease; ICFC, intracellular flow cytometry; IFN, interferon; Ig, immunoglobulin; IGRA, interferon gamma release assays; IL, interleukin; PCR, polymerase chain reaction; qPCR, quantitative polymerase chain reaction; RdRP, RNA-dependent RNA polymerase; SARS-CoV-2, severe acute respiratory syndrome coronavirus 2; TNF, tumor necrosis factor.**

Most current article

0016-5085/$36.00
https://doi.org/10.1053/j.gastro.2022.04.037

Severe acute respiratory syndrome coronavirus 2 (SARS-CoV-2) is a single-stranded positive-sense RNA virus causing respiratory, gastrointestinal, and central nervous system infections in humans collectively referred to as coronavirus disease 2019 (COVID-19).[1] Cellular SARS-CoV-2 infection is mediated by an interaction of membrane-bound angiotensin-converting enzyme 2 (ACE2) with the viral spike and is facilitated by the host proteases TMPRSS2, TMPRSS4, and CatB/L.[2] ACE2 is expressed in the brush border of enterocytes in the gut,[3] a site of SARS-CoV-2–associated inflammation.[4] Studies with intestinal epithelial organoids confirmed that SARS-CoV-2 infects human epithelium, triggering an interferon (IFN) signature.[5] Consequently, SARS-CoV-2 can be detected in anal swabs, a signal that remains positive long after nasopharyngeal swabs are negative.[6]

The postacute COVID-19 syndrome is characterized by persistent or prolonged symptoms for more than 4 weeks after acute COVID-19. Considerable disagreement about definition and, thus, prevalence of postacute COVID-19 exists, ranging from 10%–87% of patients with COVID-19.[7,8] The syndrome was initially dismissed by many but is now recognized as a multi-organ disease, which reflects a significantly growing health-care challenge.[9,10] Postacute COVID-19 typically involves symptoms including severe fatigue, cognitive dysfunction, or pain.[11] Poor baseline health status and severe acute COVID-19 convey risk for the development of postacute COVID-19, however, also mild COVID-19 (eg, in nonhospitalized patients) may culminate in postacute sequelae.[12] Although postacute COVID-19 symptoms usually do not require hospitalization,[13] disease burden weighs heavily on affected individuals.[12] Although the pathophysiological mechanisms of acute COVID-19 are well defined (eg, viral toxicity, microvascular injury, immune dysregulation, and inflammation),[1] postacute COVID-19 sequelae are poorly understood. It appears plausible that viral immune perturbation and/or inflammatory tissue injury during the acute infection account for the postacute COVID-19 syndrome.[9] For example, neural accumulation of memory T cells in COVID-19 was observed in postacute COVID-19 neuropsychiatric sequelae (eg, malaise and depression) and reflects a hallmark of immune senescence during aging and tissue injury.[9] Furthermore, it was shown that postacute COVID-19 was associated with persistently activated innate immune cells and hyperactivated T and B cells, along with increased proinflammatory cytokine expression,[14] although the cause of such prolonged immune perturbation is unknown.

Here, we took advantage of upper and lower gastrointestinal endoscopy (and related mucosal tissue availability) in patients with or without postacute COVID-19 symptoms who were evaluated in our inflammatory bowel disease (IBD) outpatient unit to explore whether gut antigen persistence[15] underlies long-term sequelae of COVID-19.

WHAT YOU NEED TO KNOW

BACKGROUND AND CONTEXT

Long-term sequelae of coronavirus disease 2019 (COVID-19), collectively termed the postacute COVID-19 syndrome, reflects a significantly growing health-care challenge. To date, the pathophysiology of this debilitating multi-organ disease is poorly understood. We investigated whether severe acute respiratory syndrome coronavirus 2 (SARS-CoV-2) antigen persistence underlies the postacute COVID-19 syndrome.

NEW FINDINGS

We report that SARS-CoV-2 antigens persist in the gut mucosa for months after acute COVID-19 in the majority of patients with inflammatory bowel disease (IBD) irrespective of immunosuppressive therapy or gut inflammation. Viral antigen persistence associates with postacute COVID-19 symptoms.

LIMITATIONS

The concept of viral antigen persistence as driver of immune perturbation and postacute COVID-19 syndrome should be corroborated in controlled clinical trials beyond IBD.

IMPACT

Collectively, our findings suggest that viral antigen persistence is a basis for postacute sequelae of COVID-19, a rapidly emerging disorder across the globe.

Methods

Study Participants and Endoscopy

In a cohort of 46 patients with IBD with polymerase chain reaction (PCR)-confirmed SARS-CoV-2 infection, we phenotyped gut tissue retrieved using upper and lower endoscopy 94–257 days (average, 7.3 months) after infection. A significant proportion of the study participants became infected in the second wave in Austria between October 2020 and February 2021 (possibly reflecting infection with the wild-type alpha and beta variant).[16] A detailed characterization of the study population is provided in Tables 1 and 2. All patients underwent endoscopy by clinical means according to IBD guidelines, and provided a negative SARS-CoV-2 PCR test at the day of endoscopic examination. We obtained biopsy specimen from the duodenum, terminal ileum, and colon (Figure 1*A*). Biopsy specimens were collected in formalin, RNAlater, or Roswell Park Memorial Institute Medium (RPMI) supplemented with 10% fetal calf serum (Sigma, St. Louis, MO). Tissue samples were further processed using SARS-CoV-2 PCR, immunofluorescence, and viral culture to analyze SARS-CoV-2 antigen persistence. All participants received a routine laboratory test and quantification of fecal calprotectin at endoscopy. Furthermore, we investigated the systemic humoral and cellular SARS-CoV-2 immune responses at time of endoscopy. Additionally, patients completed a questionnaire that recorded symptoms of the acute episode of COVID-19 and postacute COVID-19 symptoms, similar to COVID-19 vaccination status. This study was approved by the ethics committee of the Medical University Innsbruck (EK-No. 1005/2019) and informed consent was obtained from all study subjects.

SARS-CoV-2 PCR From Intestinal Biopsies

To decipher SARS-CoV-2 RNA persistence in the gastrointestinal tract, we isolated RNA as described previously.[17] In brief, RNAlater (Qiagen, Hilden, Germany)–preserved biopsy

Table 1. General Characteristics of the Study Population at Recruitment

	Mucosal SARS-CoV-2 RNA–negative	Mucosal SARS-CoV-2 RNA–positive	Overall	*P*
n	14	32	46	
Sex (%)				.36
Female	8/14 (57.1)	12/32 (37.5)	20/46 (43.5)	
Male	6/14 (42.9)	20/32 (62.5)	26/46 (56.5)	
Disease (%)				.52
Crohn's disease	9/14 (64.3)	22/32 (68.8)	31/46 (67.4)	
Ulcerative colitis	5/14 (35.7)	8/32 (25.0)	13/46 (28.3)	
IBD unclassified	0/14 (0.0)	2/32 (6.2)	2/46 (4.3)	
Metrics				
Age (*y*)	45.28 (40.93, 54.48)	44.67 (25.45, 50.58)	44.67 (28.11, 51.95)	.21
Age at IBD diagnosis (*y*)	11.05 (6.84, 14.28)	8.60 (4.99, 20.84)	9.92 (5.30, 17.38)	.75
Duration of IBD (*y*)	35.51 (28.21, 43.57)	24.96 (17.80, 37.00)	28.60 (18.49, 40.60)	.02
IBD severity (%)[a]				.13
Remission	7/14 (50.0)	20/32 (62.5)	27/46 (58.7)	
Mild	4/14 (28.6)	11/32 (34.4)	15/46 (32.6)	
Moderate	3/14 (21.4)	1/32 (3.1)	4/46 (8.7)	
Severe	0/14 (0.0)	0/32 (0.0)	0/46 (0.0)	
Crohn's disease: age at diagnosis (Montreal A) (%)[b]				.17
<16 y (A1)	0/9 (0.0)	6/22 (27.3)	6/31 (19.4)	
17-40 y (A2)	7/9 (77.8)	14/22 (63.6)	21/31 (67.7)	
>40 y (A3)	2/9 (22.2)	2/22 (9.1)	4/31 (12.9)	
Crohn's disease: behaviour (Montreal B) (%)[b]				.37
Nonconstricting & nonpenetrating (B1)	6/9 (66.7)	13/22 (59.1)	19/31 (61.3)	
Stricturing (B2)	1/9 (11.1)	7/22 (31.8)	8/31 (25.8)	
Penetrating (B3)	2/9 (22.2)	2/22 (9.1)	4/31 (12.9)	
Crohn's disease: disease location (Montreal L) (%)[b]				.25
Ileum (L1)	1/9 (11.1)	6/22 (30.0)	7/31 (22.6)	
Colon (L2)	2/9 (22.2)	1/22 (5.0)	3/31 (9.7)	
Ileum + colon (L3)	6/9 (66.7)	15/22 (68.2)	21/31 (67.7)	
Upper GI (L4)	0/9 (0.0)	0/15 (0.0)	0/31 (0.0)	
Ulcerative colitis: age at diagnosis (Montreal A) (%)[b]				.46
<16 y (A1)	0/5 (0.0)	1/8 (14.3)	1/13 (7.7)	
17-40 y (A2)	3/5 (60.0)	5/8 (71.4)	8/13 (61.5)	
> 40 y (A3)	2/5 (40.0)	1/8 (14.3)	3/13 (23.1)	
Ulcerative colitis: disease extent (Montreal E) (%)[b]				.50
Proctitis (E1)	0/5 (0.0)	0/8 (0.0)	0/13 (0.0)	
Left-sided colitis (E2)	2/5 (40.0)	6/8 (75.0)	8/13 (61.5)	
Pancolitis (E3)	3/5 (60.0)	2/8 (25.0)	5/13 (38.5)	
Risk factors and other diseases				
BMI	26.20 (21.80, 31.80)	24.50 (22.25, 26.80)	24.95 (22.20, 28.10)	.31
Smoker (%)	3/14 (21.4)	8/32 (25.0)	11/46 (23.9)	.99
Abnormality in chest x-ray (%)	4/14 (33.3)	7/32 (24.1)	11/46 (26.8)	.83
Heart disease (%)	0/14 (0.0)	2/32 (6.2)	2/46 (4.3)	.86
Diabetes (%)	1/14 (7.1)	2/32 (6.2)	3/46 (6.5)	.99
Lung disease (%)	1/14 (7.1)	1/32 (3.1)	2/46 (4.3)	.99
Kidney disease (%)	0/14 (0.0)	0/32 (100.0)	0/46 (100.0)	NA
Medication (%)				
Steroid use in last year	1/14 (7.1)	1/32 (3.1)	2/46 (4.3)	.99
Anti-TNF at endoscopy	2/14 (14.3)	12/32 (37.5)	14/46 (30.4)	.22
Ustekinumab at endoscopy	1/14 (7.1)	1/32 (3.1)	2/46 (4.3)	.99
Vedolizumab at endoscopy	1/14 (7.1)	2/32 (6.2)	3/46 (6.5)	.99
Azathioprine at endoscopy	0/14 (0.0)	4/32 (12.5)	4/46 (8.7)	.41
JAK-inhibitor at endoscopy	1/14 (7.1)	0/32 (0.0)	1/46 (2.2)	.67
5-ASA at endoscopy	4/14 (28.6)	5/32 (15.6)	9/46 (19.6)	.53
Study medication at endoscopy	2/14 (14.3)	0/32 (0.0)	2/46 (4.3)	.03

Table 1. Continued

	Mucosal SARS-CoV-2 RNA–negative	Mucosal SARS-CoV-2 RNA–positive	Overall	*P*
Medication history (%)				
History of anti-TNF	6/14 (42.9)	5/32 (15.6)	11/46 (23.9)	.11
History of Vedolizumab	3/14 (21.4)	1/32 (3.1)	4/46 (8.7)	.15
History of Ustekinumab	2/14 (14.3)	0/32 (0.0)	2/46 (4.3)	.16
History of Azathioprine	6/14 (42.9)	9/32 (28.1)	15/46 (32.6)	.53
History of JAK-inhibitor	1/14 (7.1)	0/32 (0.0)	1/46 (2.2)	.67

NOTE. Data are reported as number of subjects with percentages in parentheses or as median with interquartile range in parentheses.
5-ASA, 5-aminosalicylic acid; BMI, body mass index; JAK, Januskinase; TNF, tumor necrosis factor.
[a]IBD disease activity was assessed according to the simple endoscopic score for Crohn's disease and the Mayo Endoscopic Score for ulcerative colitis.
[b]Assessment of disease extent, disease location, and disease behavior by using the Montreal classification.[31]

specimens were homogenized in lysing buffer using a Precellys 24 Homogenisator and a Precellys Tissue RNA kit (both Bertin, Montigny-le-Bretonneux, France). Lysates were applied on RNAeasy columns (Qiagen, Hilden, Germany) and RNA extraction was carried out according to the manufacturer's instructions. Total RNA concentration was quantified at 260 nm right after isolation, using a nanodrop 1000 (Peqlab, Erlangen, Germany). RNA was stored at -80°C. RNA was transcribed to complementary DNA using an M-MLV reverse transcriptase in combination with hexamer primers (Thermo Fisher Scientific, Waltham, MA). Complementary DNA sequences were amplified by polymerase chain reaction using gene-specific primers in combination with SYBR-green chemistry to detect RNA-dependent RNA polymerase (RdRP), nucleocapsid phosphoprotein (Nucleocapsid), surface glycoprotein (Spike), and envelope protein RNA. Additionally, β-actin served as a control to validate isolation and transcription efficiency. SARS-CoV-2–specific primers were validated and extensively analyzed by Park et al[18] and are summarized in Supplementary Table 1.

Immunofluorescence

Intestinal biopsy specimens were collected in RPMI and immediately transferred in cryomolds, covered with cryostat embedding medium, and immersed in cold isopentane with liquid nitrogen until snap-frozen. Cryomolds were stored at -20°C until cryo-sectioning. For downstream immunofluorescence 4-μm cryostat sections were cut from the samples and subsequently stained for SARS-CoV-2 nucleocapsid (#PA5114448, Thermo Fisher Scientific, Waltham, MA), epithelial CK18 (#LS-B11232, LifeSpan Biosciences, Seattle, WA), CD8 (#14-0008-80, Thermo Fisher Scientific, Waltham, MA), or LGR5 (#MA5-25644, Thermo Fisher Scientific, Waltham, MA), according to a standardized immunofluorescence protocol (see Supplementary Methods). Targets were visualized with secondary fluorophore conjugated antibodies. Images were acquired on a Zeiss Axioobserver Z1 microscope in combination with a LSM700 confocal laser scanning system containing 4 lasers with 405, 488, 555, and 654 nanometre wavelengths (Zeiss, Oberkochen, Germany).

Virus Cultivation

Biopsy specimens stored in RPMI supplemented with 10% fetal calf serum at -80°C were homogenized using a Precellys 24 Homogenisator (Bertin, Montigny-le-Bretonneux, France). After homogenization the lysate was sterile filtrated and used to infect ACE-2 and TMPRSS2 overexpressing Vero cells[19] (Vero-TMPRSS2/ACE2). Three days after infection, wells were analyzed for cytopathic effect. Samples with absent cytopathic effect after 2 passages were regarded negative for infectious virus. Further details are available in the Supplementary Methods section.

Anti-SARS-CoV-2 Enzyme-Linked Immunosorbent Assays

SARS-CoV-2 spike and nucleocapsid protein specific immunoglobulins (Ig) were quantified using an anti-SARS-CoV-2 QuantiVac enzyme-linked immunosorbent assay (ELISA) (IgG) and an anti-SARS-CoV-2-NCP-ELISA (IgG) (both Euroimmun, Luebeck, Germany) according to the manufacturer's instructions. Anti-nucleocapsid Igs are categorically reported as negative, borderline, and positive, and anti-spike receptor binding domain antibody concentrations are reported as binding antibody units/mL.[20]

Cellular SARS-CoV-2 Immunity: Interferon Gamma Release Assays and Flow Cytometry

The presence of SARS-CoV-2–specific T cells directed against the spike and nucleocapsid proteins were assessed using interferon gamma release assays (IGRA) and validated with intracellular flow cytometry (ICFC).[21] To specifically stimulate SARS-CoV-2–specific T cells, lithium heparin whole blood or isolated peripheral blood mononuclear cells were coincubated with peptide pools (Miltenyi Biotech, Bergisch-Gladbach, Germany) consisting of 15-mer peptides with 11 amino acids overlap covering the entire sequence of the spike glycoprotein (pepS) and the complete sequence of the nucleocapsid phosphoprotein (pepN).

Cellular SARS-CoV-2 immunity was quantitatively analyzed using a whole blood spike IGRA and nucleocapsid IGRA,

Table 2. SARS-CoV-2–Specific Characteristics of the Study Population

	Mucosal SARS-CoV-2 RNA–negative	Mucosal SARS-CoV-2 RNA–positive	Overall	*P*
n	14	32	46	
Metrics				
Days between COVID-19 and biopsy sampling	122.00 (72.75, 236.25)	229.50 (107.25, 263.00)	218.50 (94.50, 256.75)	.17
Lung capacity				
FVC (*z* score)	-0.55 (-1.17, 0.55)	-0.64 (-1.08, -0.08)	-0.63 (-1.14, 0.32)	.97
FEV1 (*z* score)	0.54 (-0.44, 0.92)	-0.64 (-1.38, -0.03)	-0.41 (-1.17, 0.57)	.04
COVID-19 severity (%)[a]				.36
Asymptomatic	0/14 (0.0)	1/32 (3.1)	1/46 (2.2)	
Ambulatory: mild disease	12/14 (85.7)	30/32 (93.8)	42/46 (91.3)	
Hospitalized: moderate disease	1/14 (7.1)	1/32 (3.1)	2/46 (4.3)	
Hospitalized: severe disease	1/14 (7.1)	0/32 (0.0)	1/46 (2.2)	
Postacute COVID-19 symptoms (%)				
Any postacute COVID symptom	0/14 (0.0)	21/32 (65.6)	21/46 (45.7)	.001
Fatigue	0/14 (0.0)	18/32 (56.3)	18/46 (39.1)	
Memory issues	0/14 (0.0)	14/32 (43.8)	14/46 (30.4)	
Loss of smell	0/14 (0.0)	11/32 (34.4)	11/46 (23.9)	
Abdominal pain	0/14 (0.0)	10/32 (28.1)	10/46 (21.7)	
Headache	0/14 (0.0)	9/32 (28.1)	9/46 (19.6)	
Sleeping disorders	0/14 (0.0)	8/32 (25.0)	8/46 (17.4)	
Diarrhoea	0/14 (0.0)	7/32 (21.9)	7/46 (15.2)	
Persistent cough	0/14 (0.0)	7/32 (21.9)	7/46 (15.2)	
Shortness of breath	0/14 (0.0)	6/32 (18.8)	6/46 (13.0)	
Depression	0/14 (0.0)	3/32 (9.4)	3/46 (6.5)	
Palpitations	0/14 (0.0)	2/32 (6.3)	2/46 (4.3)	
Muscle pain	0/14 (0.0)	2/32 (6.3)	2/46 (4.3)	
Chest pain	0/14 (0.0)	1/32 (3.1)	1/46 (2.2)	
Rash	0/14 (0.0)	0/32 (0.0)	0/46 (0.0)	
Recurrent fever	0/14 (0.0)	0/32 (0.0)	0/46 (0.0)	
SARS-CoV-2 vaccination status (%)				
Unvaccinated	9/14 (64.3)	10/32 (31.2)	19/46 (41.3)	.08
1 dose Vaxzevria (ChAdOx1)	0/14 (0.0)	1/32 (3.1)	1/46 (2.2)	
1 dose Janssen COVID-19 Vaccine	0/14 (0.0)	1/32 (3.1)	1/46 (2.2)	
1 dose Comirnaty (BNT162b2)	0/14 (0.0)	5/32 (15.6)	5/46 (10.9)	
2 doses Vaxzevria (ChAdOx1)	0/14 (0.0)	1/32 (3.1)	1/46 (2.2)	
2 doses Spikevax (mRNA-1273)	1/14 (7.1)	6/32 (18.8)	7/46 (15.2)	
2 doses Comirnaty (BNT162b2)	2/14 (14.3)	6/32 (18.8)	8/46 (17.4)	
3 doses Comirnaty (BNT162b2)	2/14 (14.3)	2/32 (6.2)	4/46 (8.7)	
Positive PCR in medical history (%)	14/14 (100)	32/32 (100.0)	46/46 (100.0)	.99
Anti-Nucleocapsid antibodies (%)				.18
Negative	1/14 (7.1)	3/32 (9.4)	4/46 (8.7)	
Borderline	1/14 (7.1)	10/32 (31.2)	11/46 (23.9)	
Positive	12/14 (85.7)	19/32 (59.4)	31/46 (67.4)	
Anti-RBD antibodies (%)				.99
Negative	0/10 (0.0)	0/32 (0.0)	0/46 (0.0)	
Borderline	0/10 (0.0)	0/32 (0.0)	0/46 (0.0)	
Positive	14/14 (100.0)	32/32 (100.0)	46/46 (100.0)	
Nucleocapsid-specific T cells (Nucleocapsid IGRA) (%)				.75
Negative	6/14 (42.9)	17/32 (53.1)	23/46 (50.0)	
Positive	8/14 (57.1)	15/32 (46.9)	23/46 (50.0)	
Spike-specific T cells (Nucleocapsid IGRA) (%)				.99
Negative	3/14 (21.4)	7/14 (21.9)	10/46 (21.7)	
Positive	11/14 (78.6)	25/14 (78.1)	36/46 (78.3)	
Quantitative SARS-CoV-2 immunity				
Anti-RBD antibodies (BAU/mL)	274.60 (43.60, 2053.10)	809.90 (203.65, 1862.60)	658.45 (171.43, 2060.15)	.32

Table 2. Continued

	Mucosal SARS-CoV-2 RNA–negative	Mucosal SARS-CoV-2 RNA–positive	Overall	*P*
Spike-IGRA (pg/mL)	1329.05 (60.22, 2018.88)	1922.99 (299.61, 3633.77)	1707.19 (239.56, 3293.65)	.31
Nucleocapsid-IGRA (pg/mL)	45.79 (3.28, 170.75)	23.65 (0.10, 618.01)	40.38 (0.10, 455.96)	.96
Nucleocapsid immunofluorescence signal (%)				.001
Negative	14/14 (100.0)	8/32 (25)	22/46 (47.8)	
Positive	0/14 (0.0)	24/32 (75.0)	24/46 (52.2)	

NOTE. Data are reported as number of subjects with percentages in parentheses or as median with interquartile range in parentheses.
RBD, receptor binding domain.
[a]COVID-19 severity was stratified according to the World Health Organization COVID-19 clinical progression scale[32] and defined as follows: Mild, ambulatory and oxygen saturation always >90%; Moderate, hospitalization and/or decrease in oxygen saturation <90%, but no oxygen supply necessary; Severe, hospitalized and oxygen supplementation or high-flow oxygen or intubation.

respectively. Spike and nucleocapsid specific IFN-γ values were analysed using ELISA. SARS-CoV-2–specific T cells were expanded and analyzed using ICFC in a subset of patients (n = 5 without immunosuppressive therapy and n = 5 with anti-tumor necrosis factor [TNF] therapy). As in the IGRA, T cells were stimulated with pepS or pepN and analyzed on a CytoFLEX S flow cytometer (Beckman Coulter, Brea, CA) after combined surface (CD45, CD4, CD8, CD45RO, CD69) and intracellular cytokine staining (IFN–γ, TNFα, interleukin [IL]17A, granzyme B). In the IGRA and ICFC, mock- and phorbol 12-myristate-13-acetate (PMA)/Ionomycin–treated cells served as negative or positive control, respectively. Both IGRA and ICFC are further described in the Supplementary Methods section.

Statistics

Statistical significance was assumed at $P < .05$ with an unpaired 2-tailed Student *t* test, a Mann-Whitney U-test, or analysis of variance and multiple comparisons were corrected using the Sidak multiple comparison test, where appropriate. Categorical variables were analyzed using the Fisher exact test. Analysis was conducted using Prism V9 (Graphpad, San Diego, CA) and R version 4.1.0 (R Project for Statistical Computing, Vienna, Austria).

Results

SARS-CoV-2 Antigen Persistence Frequently Occurs in the Gut Mucosa

Patients recruited in this study had acute COVID-19 (PCR-confirmed SARS-CoV-2 infection) 219 days (range, 94–257) before endoscopy, which was performed to evaluate disease activity of an established IBD (ie, we did not select for patients with postacute COVID-19). At endoscopy, patients were evaluated for postacute COVID-19 symptoms (using a questionnaire) and viral antigen persistence in the gut. We included 46 patients with characteristics, comorbidities, risk factors, and medical history summarized in Table 1, and COVID-19–related clinical and biochemical characteristics shown in Table 2. Briefly, 91% (42/46) of patients had experienced mild acute COVID-19, and 45% (21/46) of patients reported at least 1 postacute COVID-19 symptom (Table 2). On the day of endoscopic examination, all patients provided a negative COVID-19 nasal or pharyngeal PCR test and did not display clinical signs of a respiratory infection. Endoscopy revealed that the majority of patients with IBD (59%) were in remission. We evaluated viral antigen persistence by analysing biopsy specimens from the small and large intestine with quantitative polymerase chain reaction (qPCR), immunofluorescence, and viral culture from gut tissue. Moreover, we evaluated a systemic SARS CoV-2–directed immune response and gut inflammation (indicated by fecal calprotectin; Figure 1*A*). Notably, 70% (32/46) of patients displayed a positive qPCR signal in at least 1 segment of the gut (ie, duodenum, ileum, or colon) (Figure 1*B*). We detected viral RNA in 31% of biopsy specimens, with expression of the RdRP in 13.6% of biopsy specimens, the surface glycoprotein (Spike) in 11.4% of biopsy specimens, the nucleocapsid phosphoprotein (Nucleocapsid) in 10.6% of biopsy specimens, and the envelope protein in 6.1% of biopsy specimens (Figure 1*C*). Detection using qPCR was unrelated to the intestinal location, the time from COVID-19 diagnosis to endoscopy, and IBD activity (Figure 1*B* and Table 2). SARS-CoV-2 expression was not detectable in stool from patients in this cohort (Supplementary Figure 1).

To confirm long-term viral antigen persistence in the mucosa and to confine the cellular localization in the gut, we performed immunofluorescence of intestinal biopsy specimens targeting the nucleocapsid phosphoprotein. The specificity of the immunofluorescence signal was confirmed in ACE2 and TMPRSS2 overexpressing vero cells infected with SARS-CoV-2 (positive control) and mucosal biopsy specimens collected in 2017, ie, before the pandemic (negative control; Supplementary Figure 2). In 52% (24/46) of patients from our cohort, we detected immunoreactivity against the viral nucleocapsid phosphoprotein in intestinal epithelial cells and immune cells in the lamina propria in the small and large intestine (Figure 2*A* and Supplementary Figure 2 and 3). Notably, all patients with a positive nucleocapsid qPCR signal (n = 13) also displayed

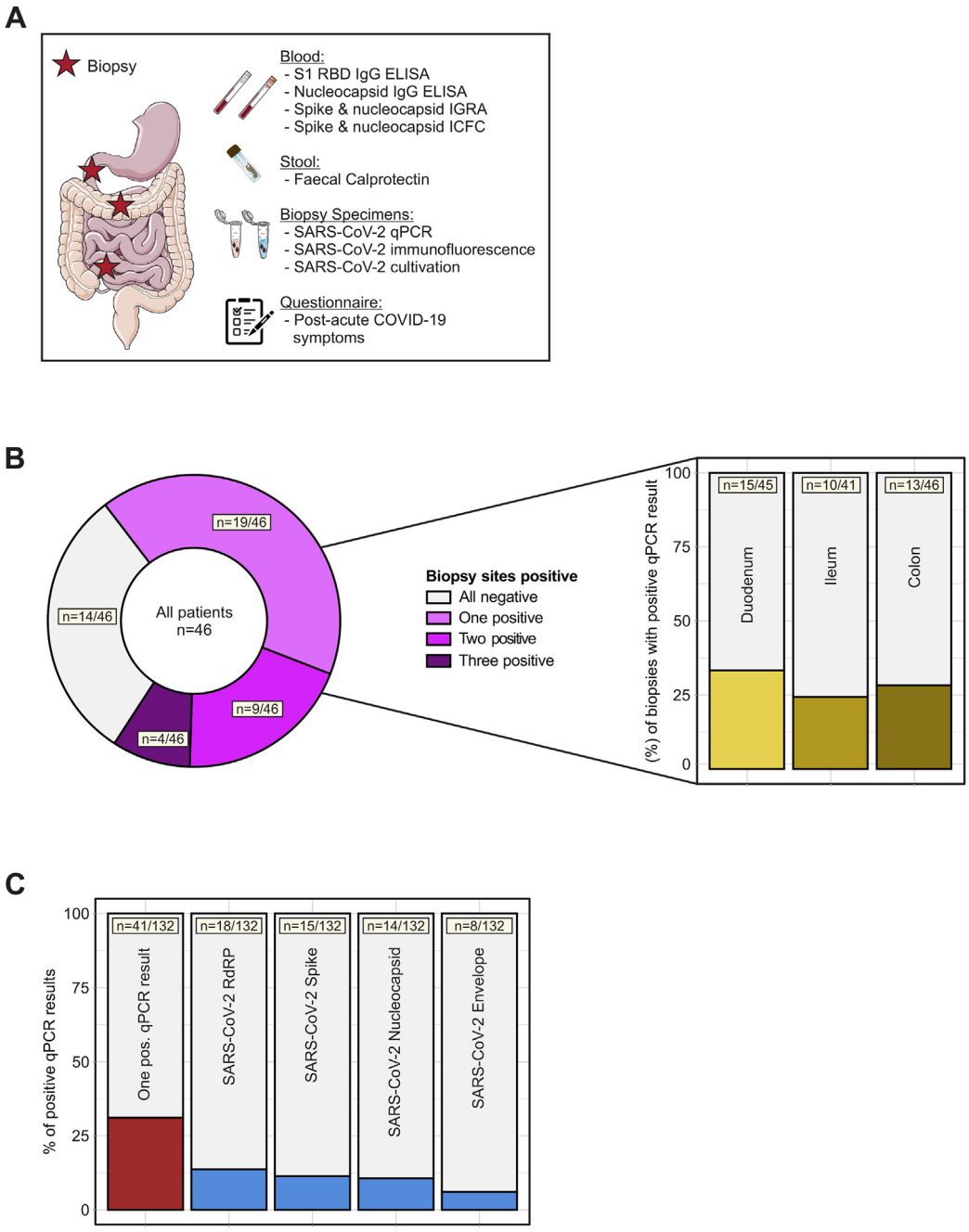

Figure 1. SARS-CoV-2 antigen persistence frequently occurs in the gut mucosa. (*A*) Study design. In a cohort of 46 patients with IBD with history of COVID-19, 219 days (range, 94–257) after the first positive PCR test endoscopy was performed and biopsy-derived tissue was phenotyped for SARS-CoV-2 mucosal antigen persistence and IBD activity. Patients were also evaluated for symptoms compatible with postacute COVID-19 sequelae using a questionnaire. The questionnaire was adapted according to the AWMF Post-Covid/long-Covid S1 guidelines,[33] and systemic SARS-CoV-2–directed immune responses were analyzed. (*B*) SARS-CoV-2 RNA was detected in 32/46 patients using qPCR. Viral RNA was detected in 1 biopsy in 19 patients, in 2 biopsies in 9 patients, and in all 3 biopsies collected in 4 patients. Detection was unrelated to the intestinal location and viral RNA was detected in 15/46 duodenal, 10/46 ileal, and 13/46 colonic samples. (*C*) Biopsies were analysed for 4 viral transcripts using qPCR (ie, RNA polymerase [RdRP], nucleocapsid phosphoprotein [Nucleocapsid], surface glycoprotein [Spike], and envelope protein). The *red bar* (*left*) indicates the proportion of biopsies with at least 1 positive qPCR signal, the *blue bars* illustrate the proportions for the respective transcript.

nucleocapsid immunoreactivity in at least 1 of 3 analyzed gut segments (Figure 2*B*). In addition, 11 patients who were RdRP-, spike-, or envelope-positive in qPCR (but without a nucleocapsid qPCR signal) displayed nucleocapsid immunoreactivity (Figure 2*B* and Table 2), indicating a patchy expression pattern as previously reported.[15] Nucleocapsid immunoreactivity specifically localized to epithelial cells (Figure 2*A*, Supplementary Figures 2 and 3), and

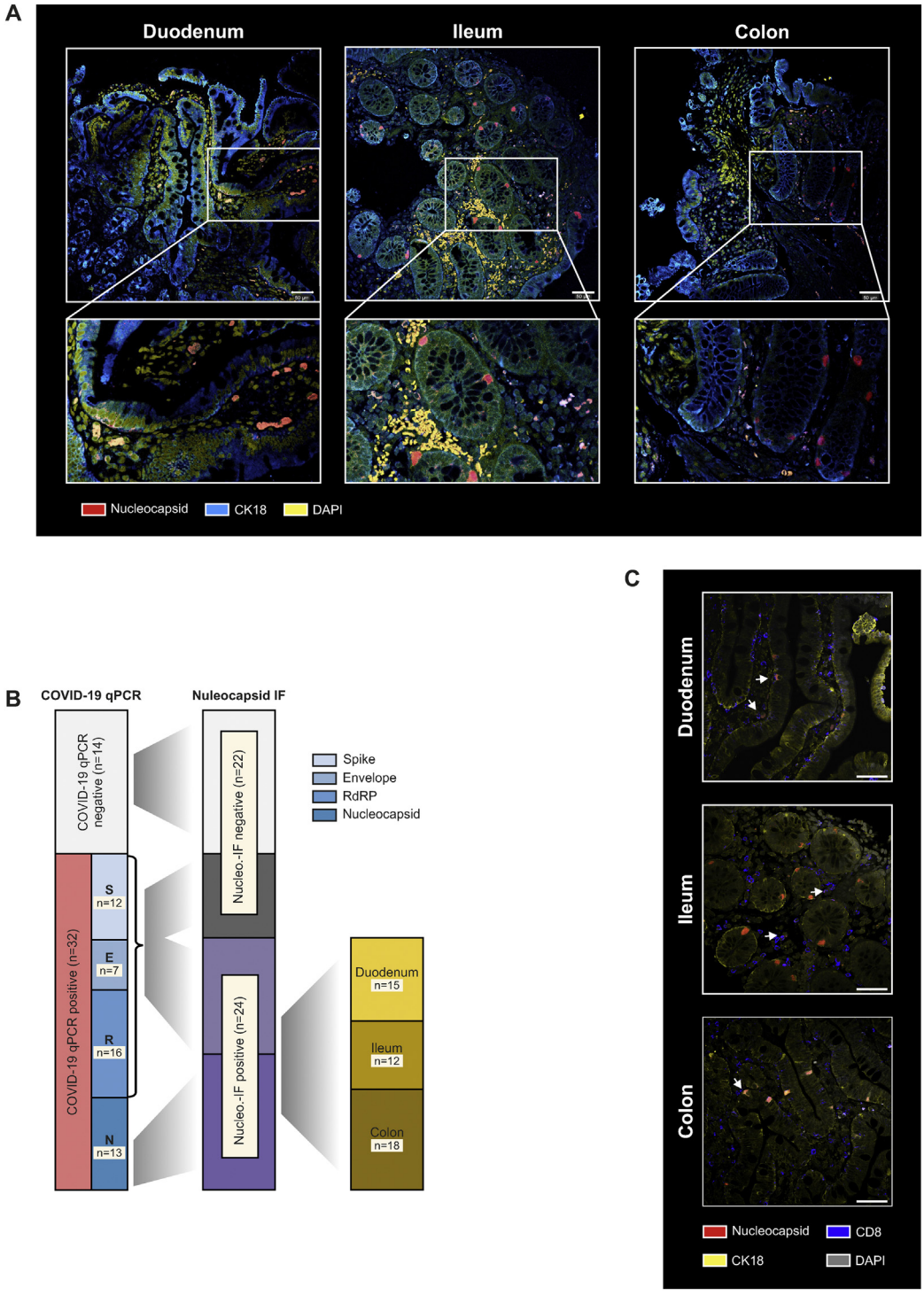

Figure 2. SARS-CoV-2 nucleocapsid immunofluorescence in the intestine. *(A)* Representative confocal microscopy images of viral nucleocapsid (*red*) in the duodenum, ileum, and colon from patients with IBD ~219 days after acute COVID-19. Cytokeratin 18 (*blue*) visualizes the epithelial cytoskeleton and 4′,6-diamidino-2-phenylindole (DAPI) (*yellow*) depicts the nucleus. Scale bar indicates 50 μm. (*B*) Association between viral qPCR positivity and antinucleocapsid immunoreactivity based on immunofluorescence. SARS-CoV-2 RNA was detected in 32/46 patients with RdRP in 16 patients, the surface glycoprotein (Spike) in 12 patients, the nucleocapsid phosphoprotein (Nucleocapsid) in 13 patients, and the envelope protein in 7 patients. All patients with a positive nucleocapsid qPCR displayed nucleocapsid immunoreactivity based on immunofluorescence in at least 1 of 3 gut segments. *(C)* Representative confocal microscopy images of viral nucleocapsid (*red*) colabelled with anti-CD8 (*blue*) in the duodenum, ileum, and colon. Cytokeratin 18 (*yellow*) visualizes the cytoskeleton and DAPI (*grey*) depicts the nucleus. Scale bar indicates 50 μm.

possibly stem cells (Supplementary Figure 4), and to a lesser extent to $CD8^+$ T cells in the epithelium and lamina propria (Figure 2*C*).

These observations led us to explore whether viral antigen persistence in the gut mucosa could be explained by SARS-CoV-2 replication. We homogenized biopsy-derived mucosal tissue from each of the 46 patients and cocultured the lysate with ACE2 and TMPRSS2 overexpressing vero cells. Although this model system showed strong replication of SARS-CoV-2 with lysates from nasal swabs of patients with symptomatic acute COVID-19, intestinal biopsy lysates from our cohort did not show evidence of replication (Supplementary Figure 5). Collectively, these data demonstrated that SARS-CoV-2 viral antigen persistence frequently occurs in the gut mucosa even months after acute COVID-19, but was not detectable in stool and appeared unrelated to viral replication.

SARS-CoV-2 Antigen Persistence Links to Postacute Sequelae of COVID-19

In a next step, we hypothesized that gut mucosal SARS-CoV-2 antigen persistence links to postacute sequelae of COVID-19. We stratified patients into 2 groups based on a positive SARS-CoV-2 qPCR result along the gut. Patients with a positive qPCR result were compared with patients who displayed no evidence for viral antigen persistence based on qPCR. Time from and disease characteristics of acute COVID-19 and IBD were comparable between both groups as shown in Tables 1 and 2 and Supplementary Table 2. Notably, only patients who displayed viral RNA expression in the gut reported symptoms compatible with postacute COVID-19 sequelae (Figure 3*A*). Patients without evidence for viral antigen persistence in our cohort ($n = 14$) did not display postacute COVID-19 symptoms (Figure 3*A*). We confirmed this observation by stratifying patients according to nucleocapsid immunoreactivity assessed using immunofluorescence (rather than qPCR positivity) (Figure 3*B*). Viral antigen persistence occurred in patients with and without immunosuppressive therapy (ie, azathioprine, anti-TNF therapy, or vedolizumab; Figure 3*C*) and was unrelated to gut inflammation indicated using fecal calprotectin (Figure 3*D* and Supplementary Table 2).

Finally, we sought to define potential mechanisms of viral antigen persistence in the intestine.[15] We analyzed SARS-CoV-2–associated humoral and cellular immune responses with ELISAs, IGRA, and by surface and ICFC of peripheral blood cells (using peptide pools mapping the spike and the nucleocapsid proteins). Blood-derived immune cells from patients with gut antigen persistence exhibited a comparable IFN-γ release on SARS-CoV-2 nucleocapsid exposure as patients without antigen persistence (Figure 3*E*). We rather noted that patients with gut viral antigen persistence more frequently lacked evidence of antinucleocapsid IgG antibodies (Figure 3*F*) and that anti-TNF immunosuppressive therapy was associated with impaired inflammatory T-cell responses on nucleocapsid peptide stimulation (Figure 3*G* and Supplementary Figure 6).

Discussion

SARS-CoV-2 infection causes acute COVID-19, ranging from asymptomatic to severe cases, partly depending on immunocompetency of the host.[22] We rationed that viral antigen persistence may underlie postacute sequelae of COVID-19. Our findings indicate that viral antigens, but not infectious virions, persist in the gut mucosa long beyond mild acute COVID-19 in patients with IBD. More specifically, antigen persistence occurs in 52%–70% of patients after ~7 months in our IBD cohort (dependent on the definition, ie, a positive nucleocapsid immunofluorescence in any gut segment, or viral RNA expression of at least 1 of 4 viral transcripts in any gut segment determined using qPCR). Viral antigen persistence of the nucleocapsid was detectable in epithelial cells and $CD8^+$ T cells in the gut. Viral antigen persistence was observed in patients with and without immunosuppressive therapy and was unrelated to severity of acute COVID-19 or gut inflammation in IBD at time of endoscopy. We argue that viral antigen persistence reflects incomplete clearance of SARS-CoV-2 rather than subclinical (latent or persistent) infection because we were unable to replicate virus from biopsy-derived tissue. In line with this, we usually detected only some (but not all) viral transcripts in biopsy specimens from the same patient. Our experimental data rather suggest that immunosuppressive therapy with or without genetic predisposition (affecting the immune system) may promote incomplete viral clearance.[23] Indeed, we find that some patients exhibit a lack of humoral nucleocapsid IgG antibodies, which is pronounced in those with gut antigen persistence. In line with this notion, a previous report demonstrated immune dysregulation, eg, a decrease of nucleocapsid-specific IFN-γ–producing $CD8^+$ T cells in patients with postacute COVID-19.[24]

To our knowledge, our study is the largest COVID-19–related gastrointestinal endoscopy study today and the first report that links viral antigen persistence with postacute COVID-19. In our report, only patients with gut antigen persistence (determined using qPCR) reported postacute COVID-19 symptoms. In contrast, none of the patients without evidence for antigen persistence in the gut reported symptoms of postacute COVID-19. This observation strongly argues for a role of viral antigen persistence in postacute COVID-19 and it appears plausible that SARS-CoV-2 antigen persistence, possibly in infected tissues beyond the gut, could impact host immune responses underlying the postacute COVID-19 syndrome.[1] This notion is supported by an influenza mouse model, demonstrating that ineffective viral clearance modulates adaptive immune responses and the formation of memory T cells in draining lymph nodes of the lung.[25] Along these lines, a recent report demonstrated that patients who survived COVID-19 pneumonia displayed long-term pulmonary $CD8^+$ T-cell alterations (although pulmonary antigen persistence was not explored).[26] Our findings also appear notable in light of the observation that T-cell activation is prolonged for 6 months in COVID-19 when compared with other acute viral infections.[27-29] In addition, a recent study revealed highly activated innate immune cells and persistent activation of T cells in individuals suffering

from postacute COVID-19, although the origin of this hyperactivated state remains obscure.[14]

Limitations of our study are the lack of a replication cohort and direct proof that SARS-CoV-2 antigen persistence affects host immune responses. Moreover, we restricted our studies to patients with IBD because it was initially conceived that this population may be particularly vulnerable to COVID-19 infection (with or without an impact on IBD activity). Our findings could be applicable to patients without IBD because viral antigen persistence has been

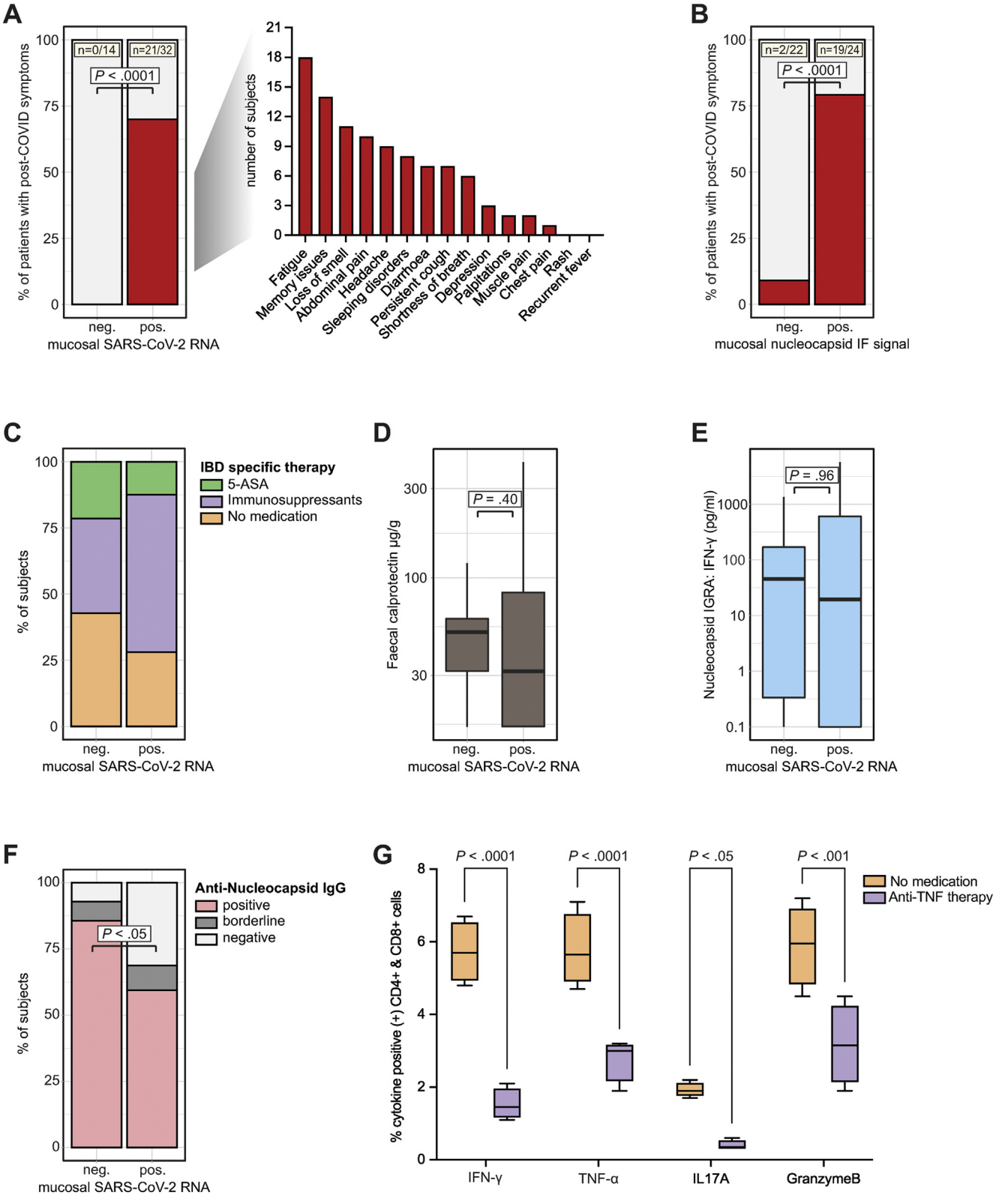

reported in the gut 2 months after COVID-19 in patients without IBD or immunosuppression.[15] Whether the reported link between gut viral antigen persistence and postacute COVID-19 is applicable to patients without IBD warrants controlled clinical trials. Our findings are also consistent with a growing body of evidence showing that COVID-19 does not affect gut inflammation in IBD.[30]

Collectively, we provide evidence for SARS-CoV-2 antigen persistence in the gut as a basis for immune perturbation in postacute COVID-19. Whether viral antigen persistence (in and beyond the gut) underlies the pathophysiology of postacute COVID-19 warrants further clinical trials to tackle this rapidly emerging disorder across the globe.[12]

Supplementary Material

Note: To access the supplementary material accompanying this article, visit the online version of *Gastroenterology* at www.gastrojournal.org, and at https://doi.org/10.1053/j.gastro.2022.04.037.

References

1. Gupta A, Madhavan MV, Sehgal K, et al. Extrapulmonary manifestations of COVID-19. Nat Med 2020;26:1017–1032.
2. Jackson CB, Farzan M, Chen B, et al. Mechanisms of SARS-CoV-2 entry into cells. Nat Rev Molec Cell Biol 2022;23:3–20.
3. Penninger JM, Grant MB, Sung JJY. The role of angiotensin converting enzyme 2 in modulating gut microbiota, intestinal inflammation, and coronavirus infection. Gastroenterology 2021;160:39–46.
4. Effenberger M, Grabherr F, Mayr L, et al. Faecal calprotectin indicates intestinal inflammation in COVID-19. Gut 2020;69:1543.
5. Lamers Mart M, Beumer J, van der Vaart J, et al. SARS-CoV-2 productively infects human gut enterocytes. Science 2020;369:50–54.
6. Wu Y, Guo C, Tang L, et al. Prolonged presence of SARS-CoV-2 viral RNA in faecal samples. Lancet Gastroenterol Hepatol 2020;5:434–435.
7. Carfì A, Bernabei R, Landi F, et al. Persistent symptoms in patients after acute COVID-19. JAMA 2020;324:603–605.
8. Greenhalgh T, Knight M, A'Court C, et al. Management of post-acute covid-19 in primary care. BMJ 2020;370:m3026.
9. Nalbandian A, Sehgal K, Gupta A, et al. Post-acute COVID-19 syndrome. Nat Med 2021;27:601–615.
10. Datta SD, Talwar A, Lee JT. A proposed framework and timeline of the spectrum of disease due to SARS-CoV-2 infection: illness beyond acute infection and public health implications. JAMA 2020;324:2251–2252.
11. Al-Aly Z, Xie Y, Bowe B. High-dimensional characterization of post-acute sequelae of COVID-19. Nature 2021;594:259–264.
12. Xie Y, Bowe B, Al-Aly Z. Burdens of post-acute sequelae of COVID-19 by severity of acute infection, demographics and health status. Nat Commun 2021;12:6571.
13. Lund LC, Hallas J, Nielsen H, et al. Post-acute effects of SARS-CoV-2 infection in individuals not requiring hospital admission: a Danish population-based cohort study. Lancet Infect Dis 2021;21:1373–1382.
14. Phetsouphanh C, Darley DR, Wilson DB, et al. Immunological dysfunction persists for 8 months following initial mild-to-moderate SARS-CoV-2 infection. Nat Immunol 2022;23:210–216.
15. Gaebler C, Wang Z, Lorenzi JCC, et al. Evolution of antibody immunity to SARS-CoV-2. Nature 2021;591:639–644.
16. Ritchie H, Mathieu E, Rodés-Guirao L, Appel Cameron, et al. Coronavirus Pandemic (COVID-19). 2020. Available at: https://ourworldindata.org/coronavirus. Accessed March 25, 2022.
17. **Zollner A, Schmiderer A, Reider SJ**, et al. Faecal biomarkers in inflammatory bowel diseases: calprotectin versus lipocalin-2-a comparative study. J Crohns Colitis 2021;15:43–54.

Figure 3. SARS-CoV-2 antigen persistence links to postacute sequelae of COVID-19. (*A*) Patients were stratified based on viral qPCR positivity in any gut segment. Patients without evident mucosal viral RNA by PCR (negative [neg.]) were compared with patients with detectable viral RNA (positive [pos.]). Proportion of patients who reported symptoms compatible with postacute COVID-19 syndrome is shown in *red*. Note that 0/14 patients without detectable mucosal viral RNA (based on qPCR in any gut segment) reported symptoms, whereas postacute COVID-19 symptoms were reported from 21/32 patients with detectable RNA (with specific symptoms listed). Statistical significance was calculated using the Fisher exact test. (*B*) Patients were stratified according to nucleocapsid immunoreactivity as assessed using immunofluorescence and data is depicted equivalent to (*A*). (*C*) Proportion of patients without IBD medication, with 5-aminosalycilates, and with immunosuppressive therapy (ie, azathioprine, anti-TNF therapy, or vedolizumab) in both groups (defined using qPCR positivity). (*D*) Quantification of fecal calprotectin concentrations in both groups (defined using qPCR positivity) using ELISA. (*E*) Quantification of SARS-CoV-2 nucleocapsid specific T-cell responses defined using IGRA (according to qPCR positivity). (*F*) Proportion of patients with positive, borderline, and negative nucleocapsid IgG in both groups (defined using qPCR positivity). Borderline and negative results were pooled, and statistical significance was calculated using the Fisher exact test. (*G*) Relative quantification of indicated cytokines defined using ICFC of T cells from patients with or without anti-TNF therapy after exposure to peptides of the SARS-CoV-2 nucleocapsid ($n = 5$). Boxplots represent median percentages of cytokine-positive $CD4^+$ and $CD8^+$ cells. Differences between groups were calculated using the Fisher exact test (*A* and *B*), 2-tailed Student *t* tests (*D*, *E*, and *F*), and 2-way analysis of variance (ANOVA) with Sidak multiple comparison post-hoc test (*G*). Boxplots represent values as median (*bold horizontal line*), interquartile range (IQR) (*box*), and 1.5 x IQR (*whiskers*). Bars represent the mean and whiskers the standard deviation.

18. Park M, Won J, Choi BY, et al. Optimization of primer sets and detection protocols for SARS-CoV-2 of coronavirus disease 2019 (COVID-19) using PCR and real-time PCR. Exp Molec Med 2020;52:963–977.
19. Riepler L, Rössler A, Falch A, et al. Comparison of four SARS-CoV-2 neutralization assays. Vaccines 2021; 9:1–13.
20. Kristiansen PA, Page M, Bernasconi V, et al. WHO International Standard for anti-SARS-CoV-2 immunoglobulin. Lancet (London, England) 2021;397:1347–1348.
21. Zollner A, Watschinger C, Rössler A, et al. B and T cell response to SARS-CoV-2 vaccination in health care professionals with and without previous COVID-19. EBioMedicine 2021;70:103539.
22. Hu B, Guo H, Zhou P, et al. Characteristics of SARS-CoV-2 and COVID-19. Nat Rev Microbiol 2021; 19:141–154.
23. McGonagle D, Kearney MF, O'Regan A, et al. Therapeutic implications of ongoing alveolar viral replication in COVID-19. Lancet Rheumatol 2022;4:e135–e144.
24. Peluso MJ, Deitchman AN, Torres L, et al. Long-term SARS-CoV-2-specific immune and inflammatory responses in individuals recovering from COVID-19 with and without post-acute symptoms. Cell Rep 2021; 36:109518.
25. Kim TS, Hufford MM, Sun J, et al. Antigen persistence and the control of local T cell memory by migrant respiratory dendritic cells after acute virus infection. J Exp Med 2010;207:1161–1172.
26. Cheon IS, Li C, Son YM, et al. Immune signatures underlying post-acute COVID-19 lung sequelae. Sci Immunol 2021;6:eabk1741.
27. **Mathew D, Giles JR, Baxter AE**, et al. Deep immune profiling of COVID-19 patients reveals distinct immunotypes with therapeutic implications. Science 2020; 369.
28. Roukens AHE, Pothast CR, König M, et al. Prolonged activation of nasal immune cell populations and development of tissue-resident SARS-CoV-2-specific CD8+ T cell responses following COVID-19. Nat Immunol 2022; 23:23–32.
29. Ryan FJ, Hope CM, Masavuli MG, et al. Long-term perturbation of the peripheral immune system months after SARS-CoV-2 infection. BMC Med 2022;20:26.
30. Lukin DJ, Funez-dePagnier G, Lima S, et al. No durable impact of COVID-19 on intestinal disease activity in subjects with IBD. Clin Gastroenterol Hepatol 2021; 19:2312–2314.e3.
31. Satsangi J, Silverberg MS, Vermeire S, et al. The Montreal classification of inflammatory bowel disease: controversies, consensus, and implications. Gut 2006; 55:749–753.
32. WHO Working Group on the Clinical Characterisation and Management of COVID-19 infection, a minimal common outcome measure set for COVID-19 clinical research. Lancet Infect Dis 2020;20:e192–e197.
33. Koczulla AR, Ankermann T, Behrends U, et al. [S1 Guideline Post-COVID/Long-COVID]. Pneumologie 2021;75:869–900.

Author names in bold designate shared co-first authorship.

Received January 18, 2022. Accepted April 20, 2022.

Correspondence
Address correspondence to: Timon E. Adolph, MD, PhD, or Herbert Tilg, MD, Department of Internal Medicine I, Gastroenterology, Hepatology, Endocrinology & Metabolism, Medical University of Innsbruck, 6020 Innsbruck, Austria. e-mail: timon-erik.adolph@i-med.ac.at or herbert.tilg@i-med.ac.at.

CRediT Authorship Contributions
Andreas Zollner, MD (Conceptualization: Equal; Data curation: Equal; Formal analysis: Equal; Investigation: Equal; Methodology: Equal; Visualization: Equal; Writing – original draft: Equal; Writing – review & editing: Equal). Robert Koch, MD (Conceptualization: Equal; Data curation: Equal; Formal analysis: Equal; Investigation: Equal; Methodology: Equal; Project administration: Equal; Validation: Equal; Writing – review & editing: Equal). Almina Jukic, MD, MSc (Conceptualization: Supporting; Data curation: Supporting; Formal analysis: Supporting; Investigation: Supporting; Methodology: Supporting; Validation: Supporting; Visualization: Supporting; Writing – review & editing: Supporting). Alexandra Pfister, BSc (Data curation: Supporting; Formal analysis: Supporting; Investigation: Supporting; Methodology: Supporting; Validation: Supporting; Visualization: Supporting; Writing – review & editing: Supporting). Moritz Meyer, MD (Data curation: Supporting; Formal analysis: Supporting; Methodology: Supporting; Writing – review & editing: Supporting). Annika Rössler, MSc (Formal analysis: Supporting; Investigation: Supporting; Methodology: Supporting; Writing – review & editing: Supporting). Janine Kimpel, PhD, MD (Formal analysis: Supporting; Investigation: Supporting; Methodology: Supporting; Writing – review & editing: Supporting). Timon Erik Adolph, PhD, MD (Conceptualization: Equal; Data curation: Equal; Formal analysis: Equal; Funding acquisition: Equal; Investigation: Equal; Methodology: Equal; Project administration: Equal; Validation: Equal; Visualization: Equal; Writing – original draft: Equal; Writing – review & editing: Equal). Herbert Tilg, MD (Conceptualization: Equal; Data curation: Supporting; Formal analysis: Equal; Funding acquisition: Equal; Investigation: Equal; Methodology: Equal; Project administration: Equal; Resources: Equal; Supervision: Equal; Validation: Supporting; Visualization: Supporting; Writing – original draft: Equal; Writing – review & editing: Equal).

Conflicts of interest
The authors disclose no conflicts.

Funding
This article received support from the European Research Council (#101039320) and the Austrian Science Fund (FWF P33070) (to T.E.A) and financial support from the Excellence Initiative (Competence Centers for Excellent Technologies [COMET]) of the Austrian Research Promotion Agency FFG: Research Center of Excellence in Vascular Ageing Tyrol, VASCage (K-Project number 843536) funded by BMVIT, BMBWF, Wirtschaftsagentur Wien, and Standortagentur Tirol (to H.T.).

Data Availability
Data will be made available after publication.

Supplementary Methods

Immunofluorescence

Intestinal biopsy specimens were collected in RPMI and immediately transferred in cryomolds, covered with OCT embedding medium, and immersed in cold isopentane with liquid nitrogen until snap-frozen. Cryomolds were stored at -20°C until cryosectioning. For downstream immunofluorescence 4-μm cryostat sections were cut from the samples and subsequently stained for SARS-CoV-2 nucleocapsid and epithelial CK18, according to a standardized immunofluorescence protocol. In brief endogenous peroxidase was blocked using Dako peroxidase block (Agilent, Santa Clara, CA). Slides were incubated with Image-iT FX signal Enhancer (#I36933, Thermo Fisher Scientific, Waltham, MA) and subsequently stained using antinucleocapsid (#PA5114448, Thermo Fisher Scientific, Waltham, MA), anti-CD8 (#14-0008-80, Thermo Fisher Scientific, Waltham, MA), anti-LGR5 (#MA5-25644, Thermo Fisher Scientific, Waltham, MA), and anti-CK18 (#LS-B11232, LifeSpan Biosciences, Seattle, WA) antibodies. Targets were visualized with secondary fluorophore conjugated antibodies. Nuclei were counterstained using ProLong Diamond antifade reagent with DAPI (Invitrogen, Carlsbad, CA); 200-μm $\times$ 200-μm images were acquired on a Zeiss Axioobserver Z1 in combination with a LSM700 confocal laser scanning system containing 4 lasers with 405, 488, 555, and 654 nanometre wavelengths (Zeiss, Oberkochen, Germany).

Virus Cultivation

Biopsy specimens stored in RPMI supplemented with 10% FCS at -80°C were homogenized using a Precellys 24 Homogenisator (Bertin, Montigny-le-Bretonneux, France).

The isolation protocol as described as follows has been established using nasal swabs from symptomatic COVID-19 patients (manuscript in preparation).

After homogenization, the lysate was sterile filtrated through spin-x columns (Corning Inc, New York, NY) and used to infect ACE-2 and TMPRSS2 overexpressing Vero cells[19] (Vero-TMPRSS2/ACE2). The inoculum was added to the cells for 1 h at 37°C, after which cells were washed once and maintained in high-glucose Dulbecco's Modified Eagle Medium (Merck, Darmstadt, Germany) supplemented with 2% FCS, 2% L-Glutamin, and 1% Penicillin-Streptomycin. Three days after infection, wells were analyzed for cytopathic effect (CPE). For wells with clear CPE, virus was harvested and frozen in aliquots at -80°C. For wells with absent or only partial CPE, a second passage was performed. Fresh confluent Vero-TMPRSS2/ACE2 cells were infected for 1 h with supernatant from the first passage. Subsequently, cells were washed and cultured for 3 days in complete medium with 2% FCS. Samples with absent CPE after 2 passages were regarded as negative for infectious virus. All work with live SARS-CoV-2 was performed in biosafety laboratory level 3 facility.

IGRA

The presence of SARS-CoV-2–specific T cells directed against the spike (S) and nucleocapsid (N) proteins were assessed using IGRA and validated with ICFC.[20] To specifically stimulate SARS-CoV-2–specific T cells, lithium heparin whole blood or isolated peripheral blood mononuclear cells (PBMC), were coincubated with peptide pools (Miltenyi Biotech, Bergisch-Gladbach, Germany) consisting of 15-mer peptides with 11 amino acids overlap covering the entire sequence of the spike glycoprotein (pepS) and the complete sequence of the nucleocapsid phosphoprotein (pepN).

For the IGRA 600-μL lithium heparin aliquots whole blood were coincubated with and without SARS-CoV-2 specific peptides. Four sample preparations were used to determine IFN-γ. One sample was mock treated to determine the steady state IFN-γ expression; in the second and third sample IFN-γ expressions were analyzed on stimulation with spike or nucleocapsid peptides (PepTivator SARS-CoV-2 ProtS, S1, S+ & N, Miltenyi, Bergisch Gladbach, Germany). An additional sample stimulated with PMA/Ionomycin served as a positive control. After 24 h on 37°C, the samples were spun down at 2000*g* for 15 min and the supernatant was stored at -80°C. Concentrations of IFN-γ were measured using a human IFN-γ ELISA kit (BD OptEIA Set Human IFNg, BD Biosciences, Pharmingen, NJ) according to the manufacturer's instructions. Negative control samples were diluted 1:5. SARS-CoV-2 peptide (pepS and pepN) coincubated samples were diluted 1:5, 1:10, and 1:15. PMA-stimulated samples were diluted 1:80 using dilution buffer. Spike and nucleocapsid reactivity were calculated by subtracting the untreated response from that of the stimulation.

ICFC

To decipher subsets of the T-cell compartment, SARS-CoV-2–specific T cells were expanded and analyzed using ICFC. First lithium heparin whole blood was collected and PBMCs were isolated using a Lymphoprep density gradient medium (Stemcell, Vancouver, Canada) according to the manufacturer's instructions. In brief, 4 mL lithium heparin blood were diluted with 3 mL phosphate buffered saline, PBMCs were isolated by layering the 7 mL on 4 mL Lymphoprep and subsequent density-gradient centrifugation for 30 min at 850*g*. PBMCs were collected from the interphase, washed twice, cryopreserved in heat-inactivated FCS supplemented with 10% dimethylsulfoxid (Sigma, St. Louis, MO), and stored in liquid nitrogen until further use.

To expand SARS-CoV-2–reactive T cells, 2 $\times$ 10^5 PBMCs in 200 μL of RPMI medium supplemented with 10% FCS were pulsed with 0.6 μg/mL spike (pepS, pepS1, and pepS+) or nucleocapsid (pepN) peptide pools in the presence of 10 U/mL interleukin-2 (IL2). Cells were cultured with IL2 only served as a negative control. After 60 h, cells were restimulated with or without 1 μg/mL spike or nucleocapsid peptide pools. Cells stimulated with 4 μg/mL phytohaemagglutinin served as positive controls. After combined surface (CD45,

CD4, CD8, CD45RO, CD69) and intracellular cytokine staining (IFN-γ, TNFα, IL-17A, granzymeB) specific T-cell responses were acquired on a CytoFLEX Flow Cytometer (Beckman Coulter, Brea, CA) and analyzed with Flowjo v10.6 (Becton Dickinson, Franklin Lakes, NJ). As in IGRA spike and nucleocapsid reactivity was calculated by subtracting the untreated response from that of stimulation. A representative gating strategy is shown in Supplementary Figure 5. Antibodies and the respective suppliers are depicted in Supplementary Table 3.

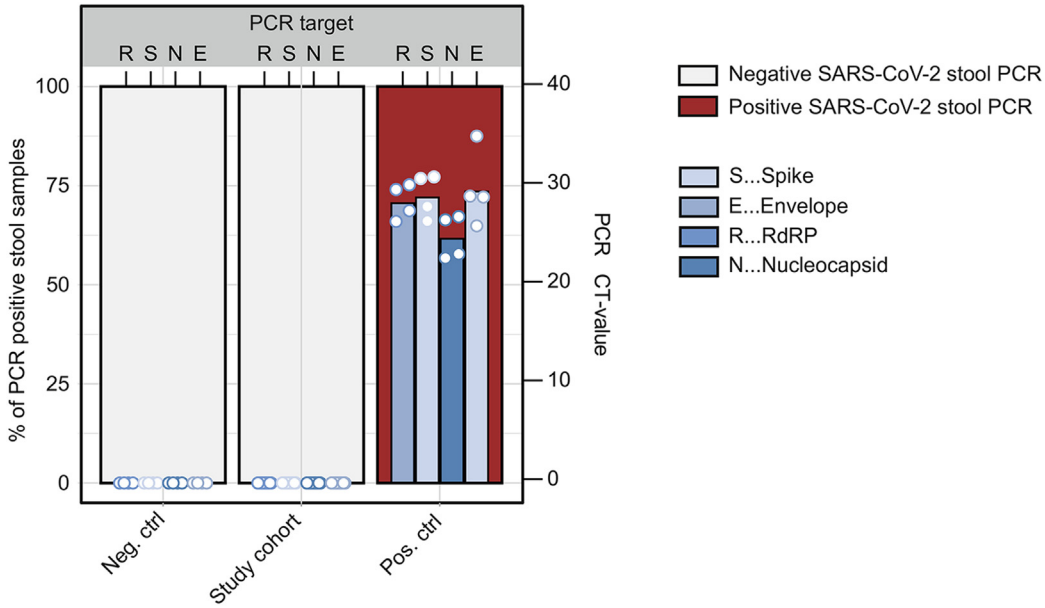

Supplementary Figure 1. Stool SARS-CoV-2 PCR. RNA was isolated from stool of patients before the pandemic (neg. ctrl; n = 4), from the study cohort (n = 46), and stool from COVID-19 subjects (pos. ctrl; n = 4). The red bars indicate percentages of samples with positive SARS-CoV-2 PCR. The blue bars show CT values for the RNA-dependent RNA polymerase (R), the spike (S), the nucleocapsid (N), and the envelope (E).

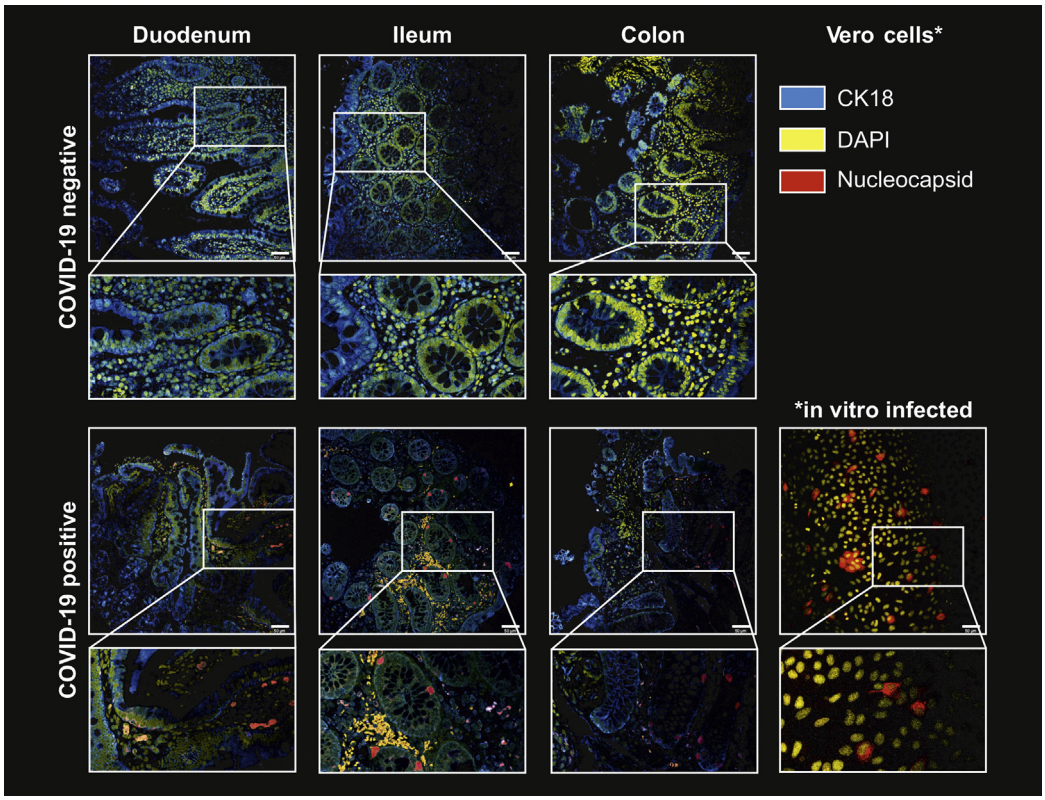

Supplementary Figure 2. SARS-CoV-2 nucleocapsid immunofluorescence of intestinal tissue. Representative confocal microscopy images of viral nucleocapsid (*red*) in the duodenum, ileum and colon mucosa from patients with IBD ~219 days after acute COVID-19 (*lower panel*). Immunostaining of sections from patients with no history of SARS-CoV-2 infection (retrieved before the pandemic) is shown in the *upper panel* and serves as a negative control. Cytokeratin 18 (*blue*) visualizes the cytoskeleton and DAPI (*yellow*) depict the nucleus. Scale bar indicates 50 μm.

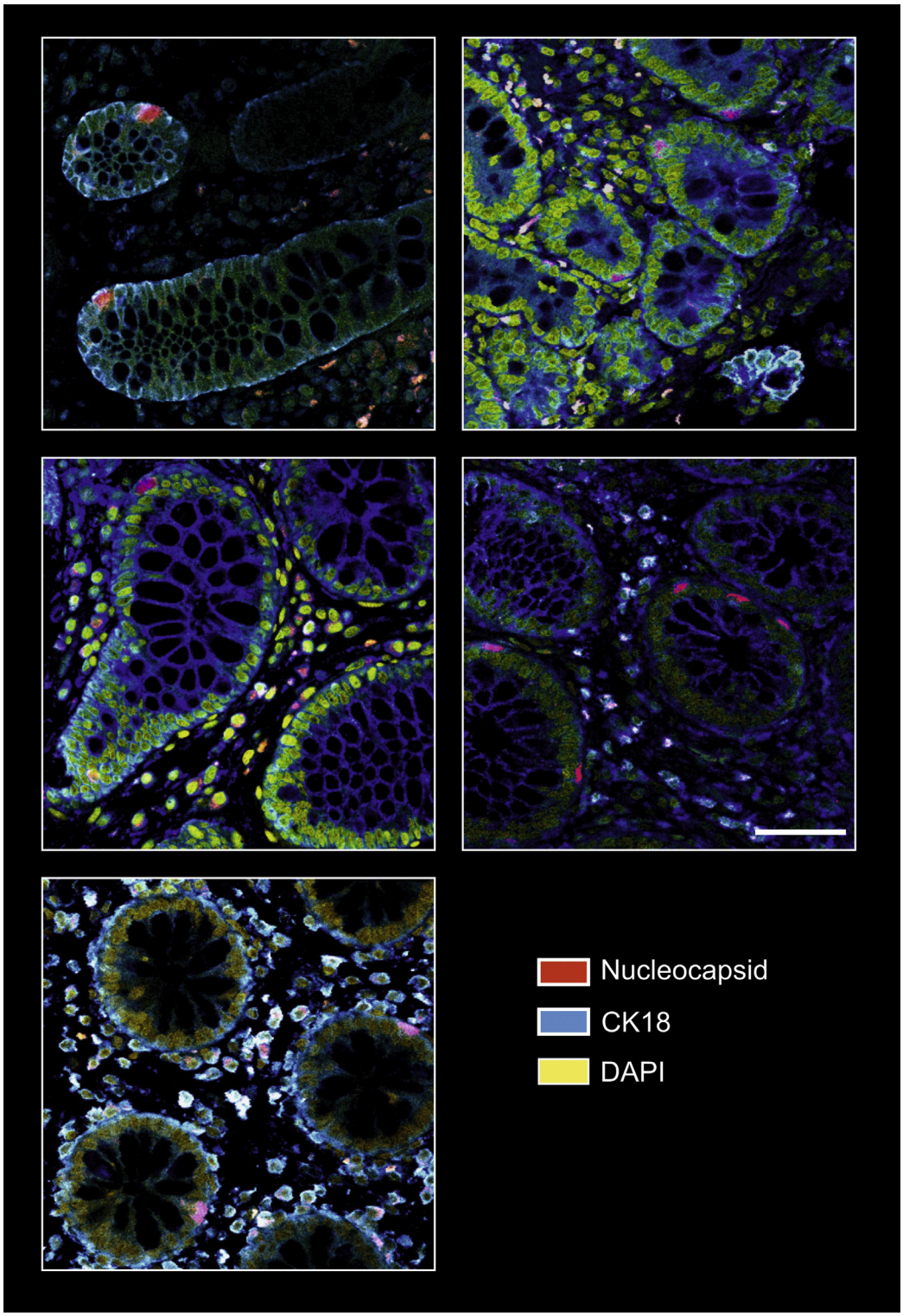

Supplementary Figure 3. Additional SARS-CoV-2 nucleocapsid immunofluorescence from intestinal tissue. As in Supplementary Figure 1, representative confocal microscopy images of viral nucleocapsid (*red*) in the duodenum, ileum, and colon mucosa from 5 patients with IBD ~219 days after acute COVID-19. Cytokeratin 18 (*blue*) visualizes the cytoskeleton and DAPI (*yellow*) depict the nucleus. Scale bar (*bottom left*) indicates 50 μm.

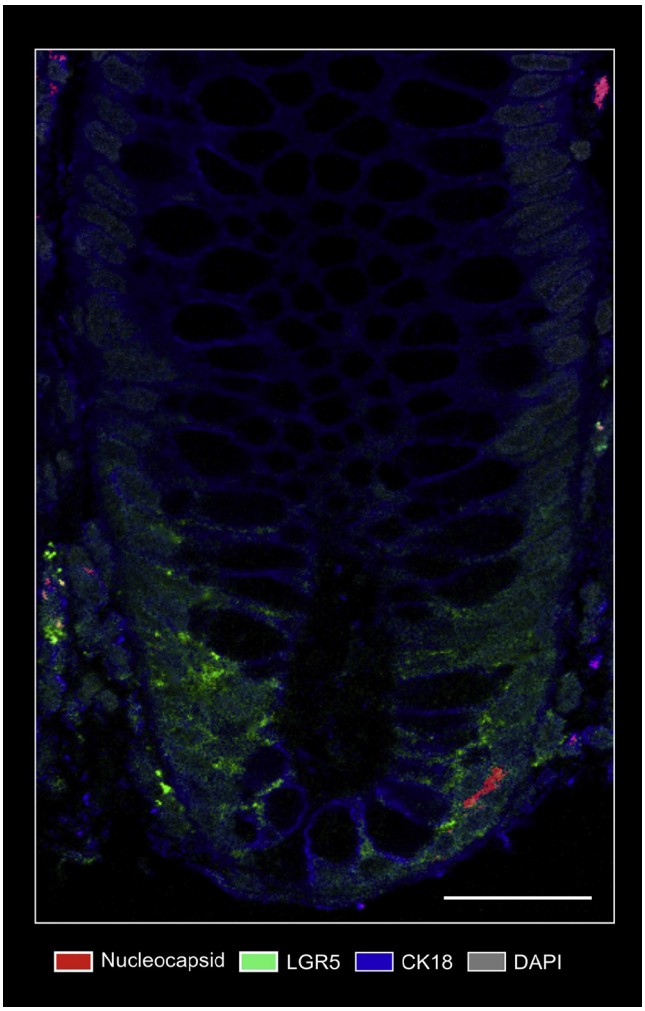

Supplementary Figure 4. Nucleocapsid/Lgr5 immunofluorescence. Representative confocal microscopy image of costainings of viral nucleocapsid (red) and Lgr5 (green) in the mucosa from a patient with IBD ~219 days after acute COVID-19. Cytokeratin 18 (blue) visualizes the cytoskeleton and DAPI (grey) depicts the nucleus. Scale bar indicates 100 μm.

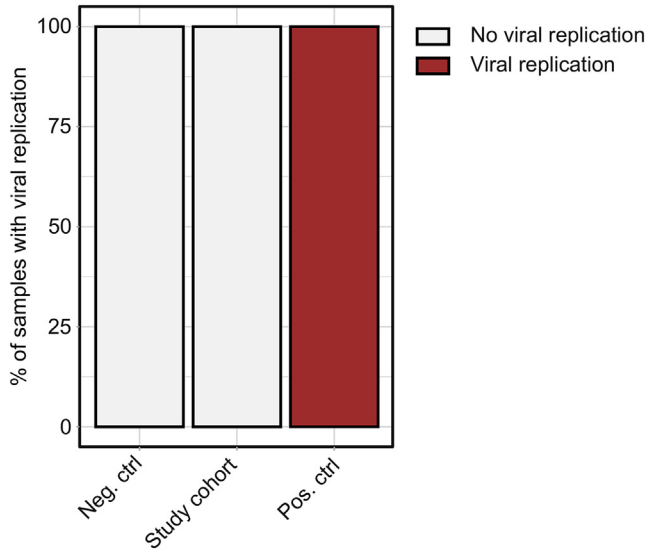

Supplementary Figure 5. SARS-CoV-2 cultivation. Lysates of negative controls (n = 4), the study cohort (n = 46), and positive controls (n = 4) were used to infect ACE-2 and TMPRSS2 overexpressing Vero cells (Vero-TMPRSS2/ACE2) and cytopathic effect was analyzed. The percentages of samples showing a cytopathic effect are indicated in *red*.

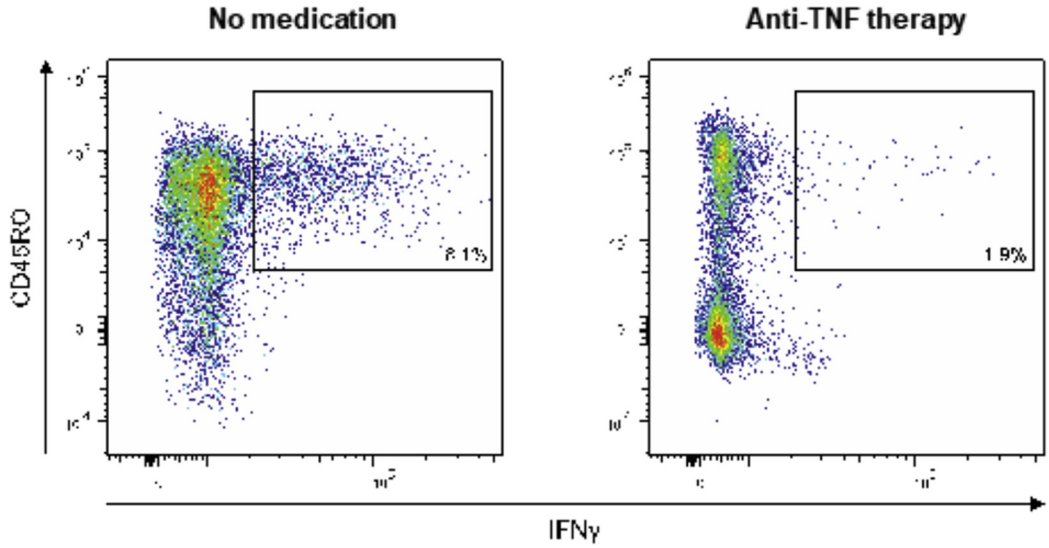

Supplementary Figure 6. Representative flow cytometry plots of cellular nucleocapsid reactivity. PBMCs were cocultivated with peptide pools covering the N protein for 60 h, restimulated, and analyzed using intracellular cytokine staining. Dot plots show $CD4^+$ and $CD8^+$ T cells that produced IFN-γ in response to stimulation nucleocapsid peptides in a patient with IBD without medication (*left*) and a patient with anti-TNF therapy (*right*).

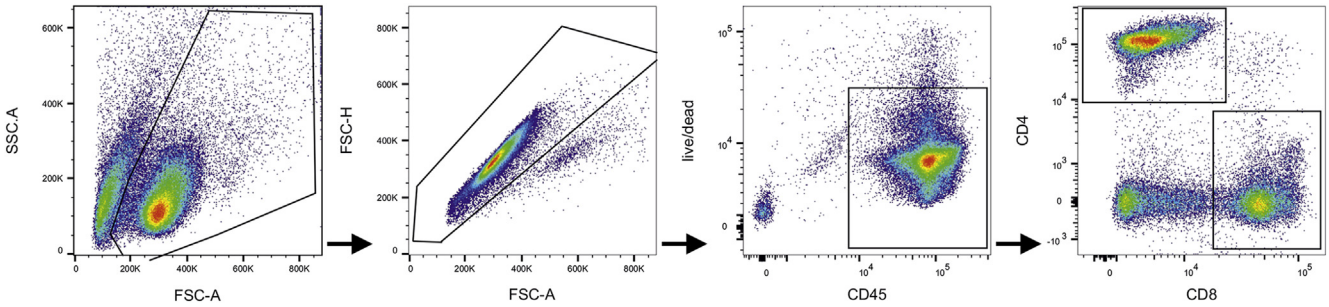

Supplementary Figure 7. Representative gating strategy. First cells were gated based on FSC and SSC; singlets were excluded by FSC-A vs FSC-H gate; live CD45$^+$ high leukocytes were gated; live CD45+ high cells were separated in CD4$^+$ and CD8$^+$ cells. These cell populations were analyzed for intracellular IFN-γ, TNFα, IL-17, and GranzymeB. FSC, forward scatter; SSC, side scatter.

Supplementary Table 1. SARS-CoV-2 and Human qPCR Primer Pairs

Target gene	Forward primer	Reverse primer
SARS-CoV-2 genes		
Surface glycoprotein	GCTGGTGCTGCAGCTTATTA	AGGGTCAAGTGCACAGTCTA
Nucleocapsid phosphoprotein	CAATGCTGCAATCGTGCTAC	GTTGCGACTACGTGATGAGG
RNA-dependent RNA polymerase	AGAATAGAGCTCGCACCGTA	CTCCTCTAGTGGCGGCTATT
Envelope protein	TTCGGAAGAGACAGGTACGTTA	AGCAGTACGCACACAATCG
Human gene		
β-actin	CACCATTGGCAATGAGCGGTTC	AGGTCTTTGCGGATGTCCACGT

NOTE. Primers were validated and extensively analyzed by Park et al.[18]

Supplementary Table 2. General Laboratory Results of the Study Population

	Mucosal SARS-CoV-2 RNA–negative	Mucosal SARS-CoV-2 RNA–positive	Overall	*P*
N	14	32	46	
General laboratory parameters				
Urea (*mg/dL*)	24.05 (21.58, 25.53)	23.05 (18.00, 27.52)	23.90 (19.27, 27.40)	.62
Creatinine (*mg/dL*)	0.81 (0.68, 0.91)	0.90 (0.75, 1.01)	0.86 (0.73, 0.97)	.09
Total bilirubin (*mg/dL*)	0.74 (0.60, 1.08)	0.92 (0.55, 1.14)	0.86 (0.56, 1.13)	.75
Sodium (*mmol/L*)	138.00 (137.00, 140.75)	139.00 (138.00, 140.00)	139.00 (138.00, 140.00)	.40
Potassium (*mmol/L*)	3.70 (3.52, 4.02)	4.00 (3.70, 4.23)	3.90 (3.62, 4.20)	.06
Chloride (*mmol/L*)	102.00 (101.25, 104.75)	103.00 (102.00, 105.00)	103.00 (102.00, 105.00)	.49
ASAT (*U/L*)	21.50 (17.25, 32.25)	24.00 (19.75, 34.25)	22.50 (18.25, 34.75)	.63
ALAT (*U/L*)	21.00 (13.25, 29.50)	23.50 (17.00, 41.00)	23.00 (17.00, 38.75)	.31
γ-GT (*U/L*)	16.50 (15.00, 28.75)	22.00 (15.75, 31.00)	20.00 (15.00, 31.25)	.39
AP (*U/L*)	81.00 (65.75, 91.00)	78.50 (63.75, 92.00)	78.50 (64.25, 91.75)	.83
LDH (*U/L*)	178.50 (164.75, 191.00)	190.00 (164.25, 201.50)	184.00 (164.25, 198.75)	.53
CRP (*mg/dL*)	0.11 (0.06, 0.25)	0.10 (0.06, 0.21)	0.10 (0.06, 0.24)	.76
Leukocytes (10^9/*l*)	6.00 (5.10, 6.27)	6.65 (5.22, 8.85)	6.25 (5.08, 8.45)	.17
Erythrocytes (10^9/*l*)	4.69 (4.35, 4.94)	4.92 (4.49, 5.31)	4.86 (4.46, 5.18)	.17
Hemoglobin (*g/L*)	136.00 (125.50, 145.50)	146.50 (138.75, 158.50)	144.50 (134.25, 153.00)	.02
Hematocrit (%)	0.40 (0.38, 0.44)	0.44 (0.41, 0.46)	0.44 (0.40, 0.46)	.02
MCH (*pg*)	28.80 (27.70, 31.40)	30.60 (29.25, 31.20)	30.25 (28.90, 31.20)	.18
MCV (*fL*)	87.80 (82.55, 92.72)	89.40 (87.53, 92.70)	88.95 (85.95, 92.70)	.36
MCHC (*g/L*)	331.00 (326.75, 339.75)	337.00 (328.00, 343.00)	336.50 (328.00, 343.00)	.27
RDW (%)	12.95 (12.75, 13.60)	12.80 (12.47, 13.20)	12.90 (12.50, 13.20)	.24
Thrombocytes (10^9/*l*)	242.00 (215.00, 297.25)	267.00 (223.75, 305.25)	262.50 (218.25, 302.75)	.50
MPV (*fL*)	10.90 (10.27, 11.60)	10.65 (9.97, 11.10)	10.75 (10.00, 11.20)	.25
Iron (μ*mol/L*)	24.25 (18.52, 33.72)	25.85 (19.62, 32.75)	25.35 (19.28, 33.05)	.80
Ferritin (μ*g/g*)	73.00 (46.50, 172.50)	124.00 (73.75, 175.75)	118.50 (60.25, 174.75)	.38
Transferrin (*mg/dL*)	269.50 (248.00, 295.50)	259.00 (236.75, 287.75)	261.50 (238.50, 289.25)	.50
Transferrin saturation (%)	36.00 (28.75, 48.75)	37.00 (28.00, 53.00)	36.00 (28.00, 53.00)	.96
Folate (μ*g/L*)	8.85 (6.20, 13.30)	8.00 (6.90, 10.00)	8.00 (6.80, 10.30)	.57
Vitamin B12	327.00 (308.75, 396.00)	293.00 (234.75, 353.75)	307.00 (237.75, 367.25)	.15
Fecal calprotectin (μ*g/g*)	51.45 (32.12, 60.48)	31.60 (16.00, 85.30)	36.95 (16.00, 69.88)	.40

NOTE. Data are reported as median with interquartile range in parentheses.
ALT, alanine transaminase; ALP, alkaline phosphatase; AST, aspartate transaminase; CRP, C-reactive protein; γ-GT, gamma-glutamyltransferase; LDH, lactate dehydrogenase; MCH, mean corpuscular hemoglobin; MCHC, mean corpuscular hemoglobin concentration; MCV, mean corpuscular volume; MPV, mean platelet volume; RDW, red cell distribution width.

Supplementary Table 3. Antibodies for ICFC

Reactivity	Fluorochrome	Supplier	RRID
CD4	Pe	Biolegend	AB_1937247
CD8	PerCP	Biolegend	AB_1575072
CD45	BV785	Biolegend	AB_2563128
CD45RO	PeDazzle	Biolegend	AB_2566542
CD69	BV605	Biolegend	AB_2562306
IFN-γ	BV421	Biolegend	AB_2561398
TNFα	APC	Biolegend	AB_315264
IL-17A	AF700	Biolegend	AB_2280255
GranzymeB	FITC	Biolegend	AB_2114575
Live/Dead	V510	Tonbo Biosciences	Not available